



**HAL**  
open science

## Temperature dependent anisotropy in the bond lengths of UO<sub>2</sub> as a result of phonon-induced atomic correlations

Lionel Desgranges, Gianguido Baldinozzi, Henry E Fischer, Gerard H Lander

### ► To cite this version:

Lionel Desgranges, Gianguido Baldinozzi, Henry E Fischer, Gerard H Lander. Temperature dependent anisotropy in the bond lengths of UO<sub>2</sub> as a result of phonon-induced atomic correlations. *Journal of Physics: Condensed Matter*, 2023, 35, pp.10LT01. 10.1088/1361-648X/acad1d . hal-03911320

**HAL Id: hal-03911320**

**<https://cnrs.hal.science/hal-03911320v1>**

Submitted on 22 Dec 2022

**HAL** is a multi-disciplinary open access archive for the deposit and dissemination of scientific research documents, whether they are published or not. The documents may come from teaching and research institutions in France or abroad, or from public or private research centers.

L'archive ouverte pluridisciplinaire **HAL**, est destinée au dépôt et à la diffusion de documents scientifiques de niveau recherche, publiés ou non, émanant des établissements d'enseignement et de recherche français ou étrangers, des laboratoires publics ou privés.

# Temperature dependent anisotropy in the bond lengths of $\text{UO}_2$ as a result of phonon-induced atomic correlations.

Lionel Desgranges<sup>1</sup>, Gianguido Baldinozzi<sup>2</sup>, Henry E. Fischer<sup>3</sup>  
and Gerard H. Lander<sup>3,4</sup>

<sup>1</sup> CEA Cadarache, IRESNE, 13108 Saint-Paul-lez-Durance, France‡

<sup>2</sup> Université Paris-Saclay, CentraleSupélec, CNRS, SPMS, 91190 Gif-sur-Yvette, France§

<sup>3</sup> Institut Laue Langevin, 71 avenue des Martyrs, CS 20156 38042 Grenoble cedex 9, France||

<sup>4</sup> European Commission, Joint Research Centre (JRC), Postfach 2340, 76125 Karlsruhe, Germany¶

22 December 2022

**Abstract.** Previous experiments on cubic  $\text{UO}_2$  have suggested that the temperature dependences of the nearest-neighbour U–O and U–U distances are *different*. We have acquired total-scattering neutron diffraction patterns out to  $Q = 23.5 \text{ \AA}^{-1}$  for  $50 < T < 1023\text{K}$  and produced via Fourier transform a pair-distribution function  $\text{PDF}(r)$ . The  $\text{PDF}(r)$  shows quite clearly that  $r(\text{U–O})$ , defined by the maximum of the U–O peak in the  $\text{PDF}(r)$ , does in fact decrease with increasing temperature, whereas  $r(\text{U–U})$  follows the lattice expansion as expected. We also observe that the  $r(\text{U–O})$  contraction accelerates continuously above  $T \approx 400 \text{ K}$ , consistent with earlier experiments by others. Furthermore, by analysing the eigenvectors of the phonon modes, we show that the  $\Delta_5(\text{TO}1)$  phonon tends to separate the eight equivalent U–O distances into six shorter and two longer distances, where the longer pair contribute to a high- $r$  tail observed in the U–O distance distribution becoming increasingly anisotropic at higher  $T$ . These results have significance for a wide range of materials in which heavy and light atoms are combined in a simple atomic structure.

## 1. Introduction

Thermal expansion is a phenomenon known to all. Although thermal expansion cannot be treated formally within the well-known harmonic approximation, and requires anharmonic potentials, the implicit assumption when a solid expands is that all the interatomic bond lengths expand in concert, or more precisely, that all average

‡ lionel.desgranges@cea.fr

§ gianguido.baldinozzi@centralesupelec.fr

|| fischer@ill.fr

¶ lander@ill.fr

interatomic distances track the overall lattice expansion monotonically. Dramatic exceptions may occur for crystalline framework structures containing rigid structural units that are flexibly bonded to each other [1, 2], or else close to the melting temperature where diffusive motion and changes in coordination number may play a strong role.

Recent experiments by Skinner [3], using total-scattering x-ray diffraction, and by Prieur et al. [4], using x-ray absorption spectroscopy, have suggested that above room temperature the well-known compound  $UO_2$  (fcc fluorite structure) exhibits an unusual anisotropy in the distance distribution of O atoms around a given U atom, such that the radius  $r(U-O)$  of the first coordination shell decreases with increasing  $T$ , whereas the U-U distance distribution remains symmetric and tracks the lattice thermal expansion. No fundamental explanation that can lead to such observations has been advanced, although molecular dynamics (MD) simulations are consistent with a U-O potential that is mostly ionic with some evidence of covalency [3, 5], a qualification that is supported by Density Functional Theory studies by Wen et al. [6].

In the present paper we report results from total-scattering neutron diffraction experiments [7, 8] using the D4 diffractometer [9] at the Institut Laue-Langevin (ILL), Grenoble, France, on a polycrystalline sample of  $UO_2$  over a range of temperature from 50 to 1023 K. Our results strongly support the earlier studies, and show additionally that the anisotropy effect in U-O distances is present at all temperatures, albeit stronger at higher  $T$ . We then give a description of the possible phonon-induced atomic correlations that could produce this effect. We suggest that such effects as reported here may exist in a large range of compounds where light and heavy atoms are combined in a simple atomic structure. The possible consequences to the materials properties, especially at higher temperatures, may prove to be significant.

## 2. Experiments

The details of the sample and neutron diffraction techniques are given in the Supplementary Information (SI). We have employed two types of diffraction data analyses. The first, and the most well-known, is that of Rietveld refinement of the diffraction patterns, i.e. considering only the integrated intensity of Bragg peaks, which consist almost entirely of elastic neutron scattering. As such, the crystallographic structure deduced from Rietveld refinement represents a time-averaged structure, following the Van Hove correlation function formalism (see also section 3). In addition, Rietveld refinement discards all diffuse scattering between Bragg peaks, such that local deviations from the long-range average structure are ignored. All this results in an atomic structure deduced from Rietveld refinement that has been averaged over time and space, which is well adapted to crystallographic considerations. Our first Rietveld results appeared to show that the oxygen atoms located at  $(\frac{1}{4}\frac{1}{4}\frac{1}{4})$  or equivalent positions are displaced from these highly symmetric coordinates towards the octahedral voids of the fluorite structure by a small distance  $\delta$  along equivalent  $\langle 111 \rangle$  directions [10], and that  $\delta$  is temperature-dependent, reaching a value of  $\delta \approx 0.017$  at 1200K. This corresponds

to a shift of  $\approx 0.16 \text{ \AA}$  from the symmetrical position ( $\delta = 0, x = \frac{1}{4}$ ). Crucially, a displacement of this magnitude in the space-time averaged structure probed by Rietveld amounts to a significant long-range static structural change that would certainly give rise to a series of new reflections at positions forbidden by the high symmetry of the fluorite lattice's fcc structure (space group  $Fm\bar{3}m$ ). Previous diffraction work on single crystals of  $\text{UO}_2$  [11, 12] have observed such ‘‘satellite’’ reflections below  $T_N (= 30 \text{ K})$ , but not above; so, this interpretation of the Rietveld results must be rejected.

Instead, we should move beyond the space-time averaged structure of Rietveld, and that brings us to our second diffraction data analysis method, known as pair-distribution function analysis (PDF-analysis), which considers all of the measured diffraction intensity, whether diffuse or not, elastic or not, and thus is qualified as a total-scattering method. Originally used for diffraction on liquids/glasses for which no long-range periodic order exists [13], PDF-analysis is now regularly applied to disordered crystalline or nano-crystalline materials [14, 15]. The diffuse scattering in diffraction results from local atomic correlations, either from static disorder or from dynamic disorder such as phonons or thermal-diffuse scattering (TDS). The  $\text{PDF}(r)$  is then obtained via Fourier transform of the total-scattering diffraction pattern (x-ray or neutron or electron) and thus retains all information about atomic positional correlations, whether static or dynamic, principally for short interatomic distances  $r$  as limited by the neutron coherence volume (about  $60 \text{ \AA}$  FWHM diameter for D4). Since a diffraction technique integrates over all energy transfers between beam and sample, its characteristic time scale of measurement is inversely proportional to the incident beam energy, and for the D4 neutron diffractometer this ‘‘snapshot time’’ is about 100 times smaller than the characteristic time of atomic motion. The  $\text{PDF}(r)$  thus represents an ensemble-average of quasi-instantaneous local atomic correlations that exist in the sample, and more precisely, the amplitude of  $\text{PDF}(r)$  is proportional to the probability of finding an atom at a distance of  $r$  from an average atom at the origin. The integrated area of a peak in  $\text{PDF}(r)$  is proportional to the coordination number at that peak position. The  $r$ -space resolution of the  $\text{PDF}(r)$  is inversely proportional to the maximum wave-vector transfer  $Q_{\text{max}}$  which for the D4 instrument is about  $23.5 \text{ \AA}^{-1}$ , giving  $\Delta r = 0.16 \text{ \AA}$  FWHM and reducing Fourier truncation effects to a minimum. Like all diffraction techniques, PDF-analysis cannot distinguish between static and dynamic correlations. At the high  $T$  for our experiments on  $\text{UO}_2$  however, it is most likely that observed changes in local atomic configurations (via PDF-analysis) are dynamic in nature, perhaps resulting from identifiable optic phonons, since long range diffusion of O should not occur in the  $T$ -range of our experiments.

We show in Fig. 1 our results for the pair-distribution function  $\text{PDF}(r)$  derived from total-scattering neutron diffraction over a broad range of temperature for a  $\text{UO}_2$  polycrystalline sample.

Our neutron diffraction  $\text{PDF}(r)$  results are in good agreement with the x-ray diffraction  $\text{PDF}(r)$  results of Skinner et al. [3] on  $\text{UO}_2$  acquired over a temperature range from  $\approx 1100 \text{ K}$  to the melting temperature ( $T_m$ ) of  $3270 \text{ K}$ , with  $Q_{\text{max}} = 21 \text{ \AA}^{-1}$ .

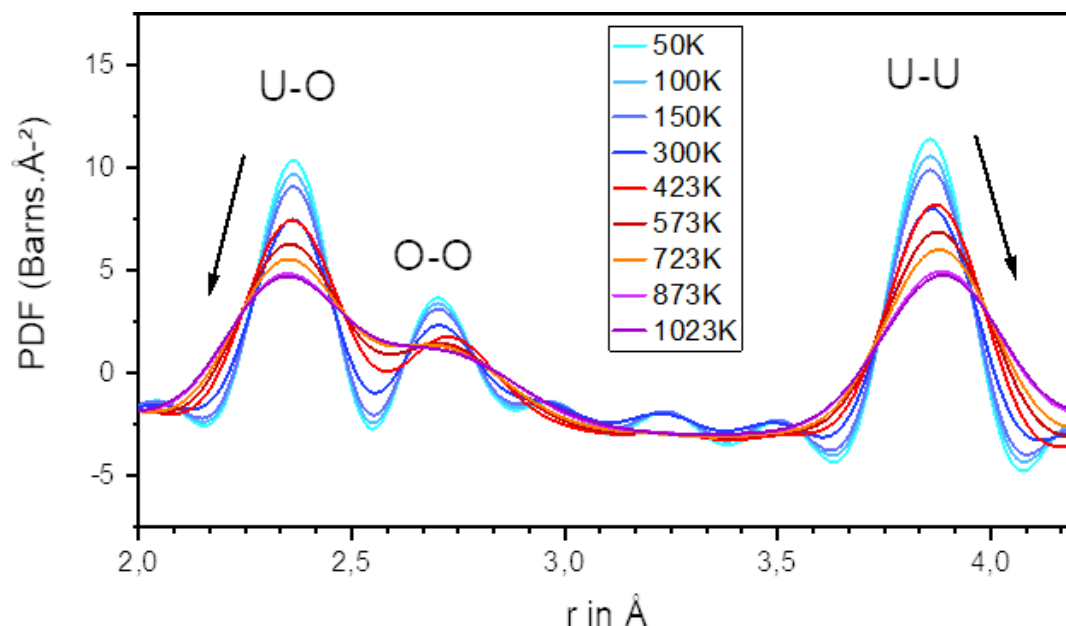


Figure 1: Neutron PDF( $r$ ) results from 50 to 1023 K. Note the increased broadening of the U–O peak with increasing temperature as it becomes more asymmetric and acquires a high- $r$  tail, all which suggests that the potential well softens and that anharmonic contributions are present. The  $r$ -space resolution is about  $0.16 \text{ \AA}$  (FWHM) for a  $Q_{\text{max}} = 23.5 \text{ \AA}^{-1}$ .

The higher incident energies of x-rays compared to neutrons allows for even shorter snapshot times, but the low- $Z$  oxygen atoms contribute much less than the U atoms to the x-ray diffraction intensity, as compared to the case of neutron diffraction. Skinner et al. [3] calculate running coordination numbers that show convincingly that the observed contraction of the first coordination shell of O atoms around an average U atom, i.e. a downward shift in the position of the  $r(\text{U-O})$  peak in PDF( $r$ ), is accompanied by a loss in members of that shell due to O atoms making excursions to higher  $r$ . Prieur et al. [4] have performed extended x-ray absorption fine structure (EXAFS) measurements on  $\text{UO}_2$  at a number of temperatures, and this technique also gives a picture of the quasi-instantaneous local structure. Their results for  $r(\text{U-O})(T)$  match those of Skinner et al. [3]. An anisotropic peak broadening of the  $r(\text{U-O})$  distribution, similar to the one observed in our experiments, was reported in a neutron total scattering experiment on  $\text{UO}_2$  at 898 K and modelled using a continuous static distribution of distances in a reverse Monte-Carlo large-box approach by Palomares et al. [16].

The different temperature dependence of the ensemble-averaged U–O and U–U distances (defined as the peak positions  $r(\text{U-O})$  and  $r(\text{U-U})$  in the PDF) is immediately evident from Figure 2. Further data analyses are described in the supplementary information. Note that the determination of  $r(\text{U-O})$  and  $r(\text{U-U})$  becomes increasingly difficult at higher  $T$ , as the peaks become very broad and overlapping – a reason we have truncated the analysis at 1023 K.

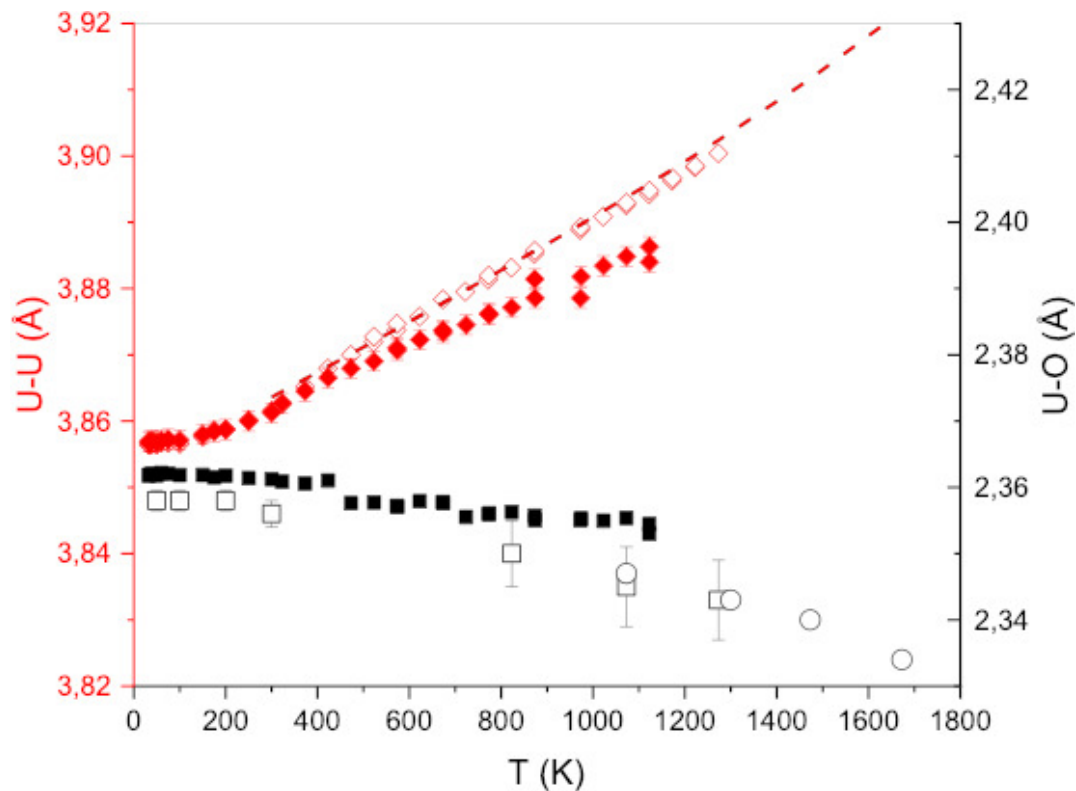


Figure 2: Experimental results for U–O and U–U distances in  $\text{UO}_2$  as determined from various techniques, as a function of temperature. Red symbols refer to U–U distance, left-hand scale. Filled diamonds: data from neutron PDF analysis. Empty diamonds; values from lattice parameters derived by Rietveld analysis of neutron data. Dashed line: values derived from x-ray lattice parameters recommended by Martin [17]. Black symbols refer to U–O distances, right-hand scale. Filled squares; values derived from neutron PDF analysis (this work). Open circles; values derived by x-ray PDF analysis and given by Skinner et al. [3]. Open squares: values derived from EXAFS experiments by Prieur et al. [4].

### 3. Model for anisotropic bond lengths

Within the Van Hove formalism, the neutron scattering amplitude of a crystal whose atoms have positional fluctuations  $\mathbf{u}_{\mathbf{R}}(t)$  (phonon amplitudes) around time-averaged positions  $\mathbf{R}$  is described by the space-time correlation function  $G(r, t)$  that can be space-Fourier transformed to the correlation function  $S(q, t)$ , which in turn can be expressed in terms of the eigenvectors of the dynamical matrix of a crystalline sample. The time-Fourier transform of  $S(q, t)$  yields  $S(q, \omega)$ , which can be measured directly by neutron or x-ray scattering. When the analysis is performed in the experimental space  $(q, \omega)$ , as for a single-crystal experiment, large spatial separations dominate the contributions to  $S(q, \omega)$ , whose oscillations therefore average out to an asymptotic value, the Debye-Waller factor. On the other hand, analysis of  $G(r, t)$  in real-space is dominated by

short-range spatial correlations of atomic positions within the coherence volume of the scattered quanta (as determined by beam optics), and the Debye-Waller factor then does not provide a good description of the positional fluctuations  $\mathbf{u}_{\mathbf{R}}(t)$ .

When phonon amplitudes are small, as in a renormalization process, the phonon self-energy modifications can, in principle, be described by perturbation theory of the anharmonic Hamiltonian expressed by a set of phonons with amplitudes  $u$  and with frequencies  $\omega$  of the unperturbed harmonic problem. The important feature of the dynamics, when we are not in a soft mode picture, is that the relevant phonon frequency is sufficiently high and it can be described by a truncated MacLaurin's series (Taylor's at  $q_0 = 0$ ) as  $\omega^2 = \omega_0^2 + \alpha^2 q^2 + \dots$ . In the classic high-temperature regime ( $k_B T \gg \hbar\omega$ ) the phonon amplitude  $u$  can be derived from the fluctuation-dissipation theorem:

$$\langle u^2 \rangle \propto \frac{k_B T}{\omega_0^2 + \alpha^2 q^2} \quad (1)$$

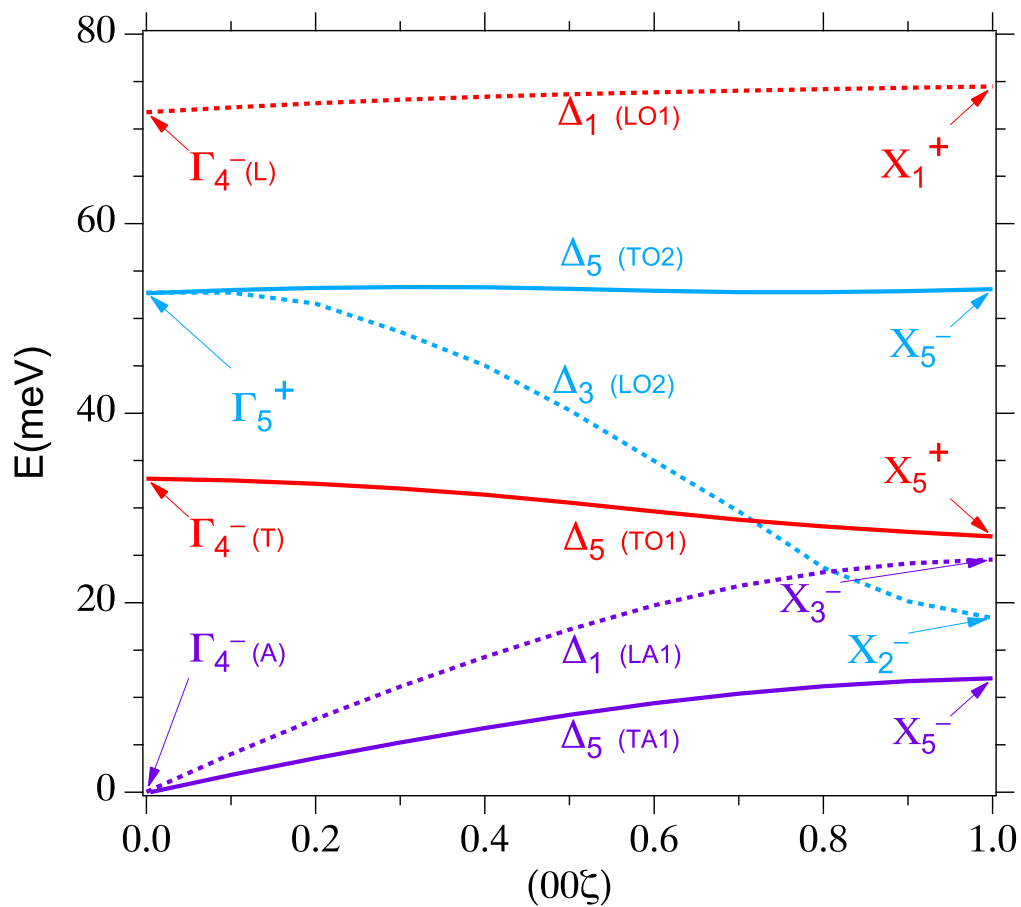
The correlation function of the amplitudes of the phonon  $u$  at two atom sites  $i$  and  $j$  is then given by the Ornstein-Zernike function:

$$\langle u_i u_j \rangle \propto \frac{1}{\|\mathbf{R}_i - \mathbf{R}_j\|} \exp \left[ \frac{-\omega_0 \|\mathbf{R}_i - \mathbf{R}_j\|}{\alpha} \right] \quad (2)$$

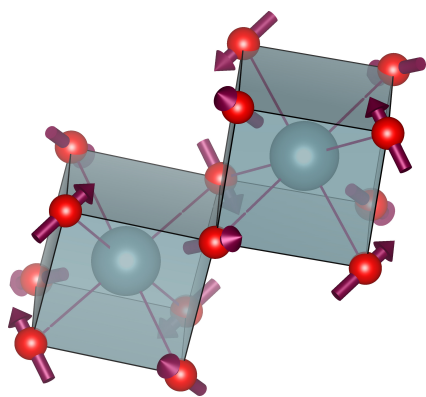
and here the correlation length  $\xi = \frac{\alpha}{\omega_0}$  decreases with increasing phonon frequency. For this reason, even if all phonons become active at high temperature and contribute to the total phonon density of states, the weakly dispersing low-energy phonons contribute the most to correlated displacements, whereas the atomic correlations from higher-energy phonons can be safely described as uncorrelated. An estimate of the correlation length  $\xi$  can be obtained for the zone-boundary: for an optic band having a dispersion  $\gamma$  and lattice parameter  $a$ , we have  $\xi \rightarrow \frac{a}{\pi} \sqrt{\frac{2\gamma}{\omega_0}}$ , which amounts to a few Å. This means that in a total-scattering experiment (as we have performed) the atomic correlations resulting from these dynamic positional fluctuations contribute to the pair-distribution function PDF( $r$ ) at distances rarely exceeding the third neighbours.

The phonon dispersion curves for  $UO_2$  were first measured in pioneering experiments in 1965 by Dolling et al. [18] More recently, the phonons (and their linewidths) have been measured as a function of temperature up to 1200 K. We reproduce in Figure 3a the phonon modes along the [001] direction as measured by Pang et al. [19].

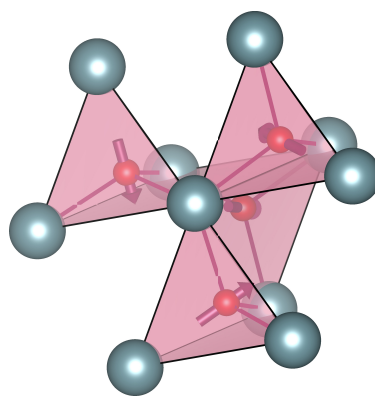
The only vibrational modes in the figure with energy  $< 40$  meV are the acoustic bands ( $\Delta_1$  and  $\Delta_5$ ), a fraction of the highly dispersive  $\Delta_3$  branch, and the weakly dispersing  $\Delta_5$  branch related to the IR-active transverse mode. The phonon density of states (PDOS) measured at 295 K and 1200 K (Figures 1 and 2 in Pang et al. [20]) actually show a series of peaks in the vibrational PDOS, one of which is close to 35 meV. The highly dispersive components with a longitudinal character do not contribute effectively to the correlated-amplitude features (branches  $\Delta_1$  and  $\Delta_3$ ), whereas the two doubly degenerate transverse branches ( $\Delta_5$ ) (TO1 and TO2) can provide some correlated-amplitude contributions. In particular, this is the case of the weakly dispersing  $\Delta_5$  branch going from  $\Gamma_4^-$  to  $X_5^+$  (TO1) at about 30 meV that provides



(a)



(b)



(c)

Figure 3: *a)* Schematic of phonon dispersion curves, as measured by Pang et al. [19] in the  $[001]$  direction. *b)* Schematic representation of the correlated displacements of the oxygen atoms generated by the  $X_5^+$  phonon at the  $X$ -point. In this figure, the octahedral coordination around each uranium atom (larger gray spheres) is emphasized. *c)* Schematic representation of the correlated displacements of the oxygen atoms generated by the  $X_5^+$  phonon at the  $X$ -point. In this figure, the tetrahedral coordination around each oxygen atom (smaller red spheres) is emphasized.

the strongest contribution to the correlated-amplitude effects in the total scattering pair-distribution function. Most of this contribution seems to originate from phonons close to the  $X_5^+$  point.

The atomic displacements corresponding to the phonon branches  $X_5^+$  at the  $X$ -point see the uranium atoms at rest, whereas the O atoms vibrate along  $\langle 111 \rangle$  directions. The displacements are schematically displayed in Figs. 3b and 3c, where we see that the octahedral voids of the fluorite structure permit such vibrational excursions along  $\langle 111 \rangle$ .

The crucial importance of the  $X_5^+$  phonon is that its action results in a separation of the U–O bonds into two different lengths. Assuming a lattice parameter of 5.47 Å, the eight U–O distances in the radial distribution function are initially at 2.3685 Å ( $a\sqrt{\frac{3}{4}}$ ) and the O–O distances at 2.735 Å ( $a/2$ ). Assuming an amplitude of  $0.0053 \cdot [111]$  (equivalent to a displacement of 0.05 Å) for the correlated displacements of the O atoms, there are six U–O distances at 2.35 Å and two at 2.415 Å, thus shortening and skewing the distance distribution, whereas the peak of the O–O distances is only slightly changed. Furthermore, as the U atoms are at rest, the U–U distances are unaffected by this phonon correlation.

#### 4. Discussion and Conclusion

Our neutron PDF( $r$ ) results for  $UO_2$  strongly support the earlier x-ray PDF( $r$ ) results by Skinner et al. [3] as well as the EXAFS results by Prieur et al. [4]. All three techniques measure an ensemble-average of quasi-instantaneous local atomic structures, and all three show that  $r(\text{U–O})$ , corresponding to the peak in the nearest-neighbor U–O distance distribution, decreases with increasing  $T$  as the distribution becomes asymmetric (see Figures 1 and 2). In contrast, the U–U distance distribution remains symmetric, and  $r(\text{U–U})$  increases as expected with  $T$ . We have presented a plausible model for these observations, based on the eigenvectors of the phonon modes, showing that the  $\Delta_5$  transverse optic phonon is capable of splitting the eight nominally equivalent U–O distances (see Fig. 3) into a bimodal distribution that has six O atoms at a slightly shorter-than-nominal distance, and two O atoms at a slightly longer-than-nominal distance, as they make vibrational excursions along  $\langle 111 \rangle$  towards the octahedral voids of the fluorite structure. Although a dynamic process, this distance splitting is clearly visible in the x-ray and neutron PDF( $r$ ) as an increasingly asymmetric U–O distance distribution acquiring a high- $r$  tail as  $T$  increases. We find that the contraction of the first U–O coordination shell represented by  $r(\text{U–O})$  accelerates above  $\approx 400$  K, which corresponds well to an increase in the population of the  $\Delta_5$  transverse optic phonon having energy  $\approx 35$  meV ( $\approx 400$  K).

Asymmetric/anisotropic nearest-neighbour distance distributions due to atomic vibrations are indicative of anharmonic potentials, and it is well known that anions in the fluorite structure are subject to such potentials. These effects manifest themselves as modifications of the Debye-Waller factors observed in Bragg peak refinement methods,

as was first detected in  $CaF_2$  itself by Strock & Batterman [21]. Willis and collaborators found similar effects in  $UO_2$  [22]. Interestingly, Willis initially interpreted the single-crystal neutron data with a model having a displacement of the O atoms along  $\langle 111 \rangle$  in the space-time average structure, i.e. measurable in Bragg peak intensities [23]. However, as we have discussed in Section 2, this interpretation predicts new Bragg reflections, which have never been observed. Anharmonicity also has other consequences that have been observed, noticeably a strong broadening of the phonon linewidths as a function of temperature [19, 20], as well as effects on the vibrational entropy and specific heat [24].

Anion amplitudes of low frequency optical phonons were singled out as an important ingredient to assist superionic conduction in binary and ternary compounds [25]. Whereas Wakamura's model addresses specifically diffusion and the behaviour of zone-centre phonons, it can be straightforwardly extended to phonons at the zone boundary that are relevant to the present study. The parameter with specific importance is the damping constant of the vibrational modes involving only displacements of the anions. This is indeed the specific configuration of  $X_5^+$  phonon, and of part of the related  $\Delta_5$  branch. Following Wakamura's arguments, in systems with large anions (as O ions) the damping constant for cations is significantly smaller than the one for anions. The direct consequence of the model is a specific and significant broadening of the phonons involving anion displacements compared to modes involving the heavier cations. In real space, this translates into an increased capacity of O ions to ramble around their equilibrium positions. The predicted behaviour of zone-centre modes correlates with this model in many superionic conductors, and, not surprisingly, the extension to zone-boundary correlates impressively with the present case of  $UO_2$  as well. Indeed, Pang et al. [20] provide irrefutable experimental evidence that the  $\Delta_5$  branch and in particular  $X_5^+$  is overdamped, whereas the other phonon branches behave normally. These zone boundary effects agree with the extension of Wakamura's model.

We do not imply that the current effect is related to a superionic transition, because the model is applied to phonons at different points of the Brillouin zone, but the two effects share some common ingredients. Therefore, we can reasonably assume that the correlation effects discussed in this paper are not specific to  $UO_2$ , but rather relevant to a broader class of systems that can have an intersection with ionic conductors, in particular with those that involve large anions and cations.

## References

- [1] Andrew L. Goodwin, Mark Calleja, Michael J. Conterio, Martin T. Dove, John S. O. Evans, David A. Keen, Lars Peters, Matthew G. Tucker, Colossal Positive and Negative Thermal Expansion in the Framework Material  $Ag_3[Co(CN)_6]$ , *Science* 319, 794 (2008).
- [2] M. G. Tucker, D. A Keen, J S O Evans and Martin T Dove, Local structure in  $ZrW_2O_8$  from neutron total scattering, *J. Phys. Condens. Matter* 19, 335215 (2007).
- [3] L. B. Skinner, C. J. Benmore, J. K. R. Weber, M. A. Williamson, A. Tamalonis, A. Hebden, T. Wiencek, O. L. G. Alderman, & M. Guthrie, L. Leibowitz, J. B. Parise, Molten uranium dioxide structure and dynamics, *Science* 346, 984-987 (2014).

- [4] D. Prieur, E. Epifano, K. Dardenne, J. Rothe, C. Hennig, A. C. Scheinost, D. R. Neuville, and P. M. Martin, Peculiar Thermal Behavior of  $UO_2$  Local Structure, *Inorg. Chem.* 57, 14890–14894 (2018).
- [5] C. J. Benmore et al., Topological ordering in liquid  $UO_2$ , *J. Phys.: Condens. Matter* 28, 015102 (2016).
- [6] Xiao-Dong Wen, Richard L. Martin, Thomas M. Henderson, and Gustavo E. Scuseria, Density Functional Theory Studies of the Electronic Structure of Solid State Actinide Oxides, *Chemical Reviews* 113, 1063 (2013).
- [7] L. Desgranges, G. Baldinozzi, Henry E. Fischer; Ph. Garcia, M.A. Yue and D. Simeone, Characterisation of cuboctahedra in  $UO_{2+x}$  as function of temperature (beamtime proposal), (2014). Institut Laue-Langevin (ILL) doi:10.5291/ILL-DATA.6-06-453
- [8] L. Desgranges, R. Caciuffo, Henry E. Fischer; Ph. Garcia and G. Lander, Local atomic and magnetic order in uranium oxide at low temperature (beamtime proposal), (2018). Institut Laue-Langevin (ILL) doi:10.5291/ILL-DATA.6-06-471
- [9] H.E. Fischer, G.J. Cuello, P. Palleau, D. Feltin, A.C. Barnes, Y.S. Badyal and J.M. Simonson, D4c: A very high precision diffractometer for disordered materials, *Appl. Phys. A* 74, S160–S162 (2002).
- [10] L. Desgranges, Y. Ma, Ph. Garcia, G. Baldinozzi, D. Simeone, and H. E. Fischer, What Is the Actual Local Crystalline Structure of Uranium Dioxide,  $UO_2$ ? A New Perspective for the Most Used Nuclear Fuel, *Inorg. Chem.* 56, 321–326 (2017).
- [11] J. Faber and G. H. Lander, Neutron diffraction study of  $UO_2$ . Antiferromagnetic state, *Phys. Rev. B* 14, 1151–1164 (1976).
- [12] S. B. Wilkins, R. Caciuffo, C. Detlefs, J. Rebizant, E. Colineau, F. Wastin, and G. H. Lander, Direct observation of electric-quadrupolar order in  $UO_2$ , *Phys. Rev. B* 73, 060406(R) (2006).
- [13] H.E. Fischer, A.C. Barnes and P.S. Salmon, Neutron and x-ray diffraction studies of liquids and glasses, *Rep. Prog. Phys.* 69, 233 (2006).
- [14] Egami, T.; Billinge, S. J. L. *Underneath the Bragg peaks: structural analysis of complex materials*, 2nd ed.; Elsevier: Amsterdam, 2012.
- [15] Maxwell W. Terban and Simon J. L. Billinge, Structural Analysis of Molecular Materials Using the Pair Distribution Function, *Chemical Reviews* 122, 1208 (2022).
- [16] Raul I. Palomares, Marshall T. McDonnell, Li Yang, Tiankai Yao, Jennifer E. S. Szymanowski, Joerg Neufeind, Ginger E. Sigmon, Jie Lian, Matthew G. Tucker, Brian D. Wirth, and Maik Lang, Oxygen point defect accumulation in single-phase  $UO_{2+x}$ , *Phys. Rev. Mat.* 3, 053611 (2019).
- [17] D. G. Martin, The thermal expansion of solid  $UO_2$  (and (U, Pu) mixed oxides – a review and recommendations, *J. Nucl. Mats.* 152, 94–101 (1988).
- [18] G. Dolling, R. A. Cowley, and A. B. D. Woods, The crystal dynamics of uranium dioxide, *Can. J. of Phys.* 43, 1397–1413 (1965).
- [19] J. W. L. Pang, W. J. L. Buyers, A. Chernatynskiy, M. D. Lumsden, B. C. Larson, and S. R. Phillpot, Phonon Lifetime Investigation of Anharmonicity and Thermal Conductivity of  $UO_2$  by Neutron Scattering and Theory, *Phys. Rev. Lett.* 110, 157401 (2013).
- [20] J. W. L. Pang, A. Chernatynskiy, B. C. Larson, W. J. L. Buyers, D. L. Abernathy, K. J. McClellan, and S. R. Phillpot, Phonon density of states and anharmonicity of  $UO_2$ , *Phys. Rev. B* 89, 115132 (2014).
- [21] H. B. Strock and B. W. Batterman, X-ray study of anharmonic vibrations in calcium fluoride. *Phys. Rev. B* 5, 2337 (1972).
- [22] B. T. M. Willis and R.G. Hazell, Re-analysis of Single-Crystal Neutron-Diffraction Data on  $UO_2$  Using Third Cumulants, *Acta Cryst.* A36, 582 (1980).
- [23] B. T.M Willis, Neutron diffraction studies of the actinide oxides II Thermal motions of the atoms in uranium dioxide and thorium dioxide between room temperature and 1100 C, *Proc. R. Soc. London Ser. A* 274, 134–144, (1963).

- [24] M. S. Bryan, J. W. L. Pang, B. C. Larson, A. Chernatynskiy, D. L. Abernathy, K. Gofryk, and M. E. Manley, Impact of Anharmonicity on The Vibrational Entropy and Specific Heat of  $UO_2$ , *Phys. Rev. Matls.* 3, 065405 (2019).
- [25] K. Wakamura. Roles of phonon amplitude and low-energy optical phonons on superionic conduction. *Phys. Rev. B* 56, 11593-11599 (1997).